Elucidating the Effect of Lead Iodide Complexation Degree behind Morphology and Performance of Perovskite Solar Cells

Rosanna Mastria, Silvia Colella, Antonio Qualtieri, Andrea Listorti, Giuseppe Gigli and Aurora Rizzo

Istituto di Nanotecnologia CNR-Nanotec, Polo di Nanotecnologia c/o Campus Ecotekne, Via Monteroni 73100 Lecce, Italy

Dipartimento di Matematica e Fisica "E. De Giorgi", Università del Salento, Via per Arnesano, 73100 Lecce, Italy

Center for Bio-Molecular Nanotechnology - Fondazione Istituto Italiano di Tecnologia IIT, Via Barsanti, 73010 Arnesano (Lecce), Italy

Supporting Information

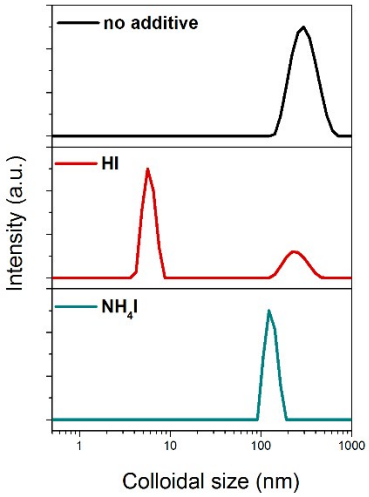

Figure S1. Dynamic light scattering profiles of pristine MAI and PbI_2 binary precursor mixture (black line), and MAI and PbI_2 added with 0.3 equivalent of HI (red line) and 0.8 equivalent of NH_4I (green line).

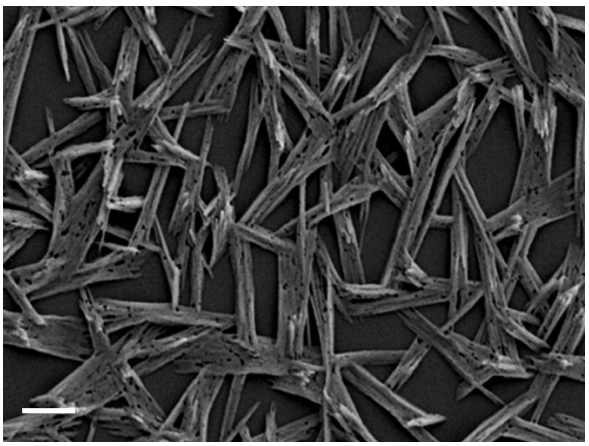

Figure S2. SEM image of $MAPbI_3$ thin film prepared from a standard binary mixture of MAI and PbI_2. Scale bar is 2 µm.

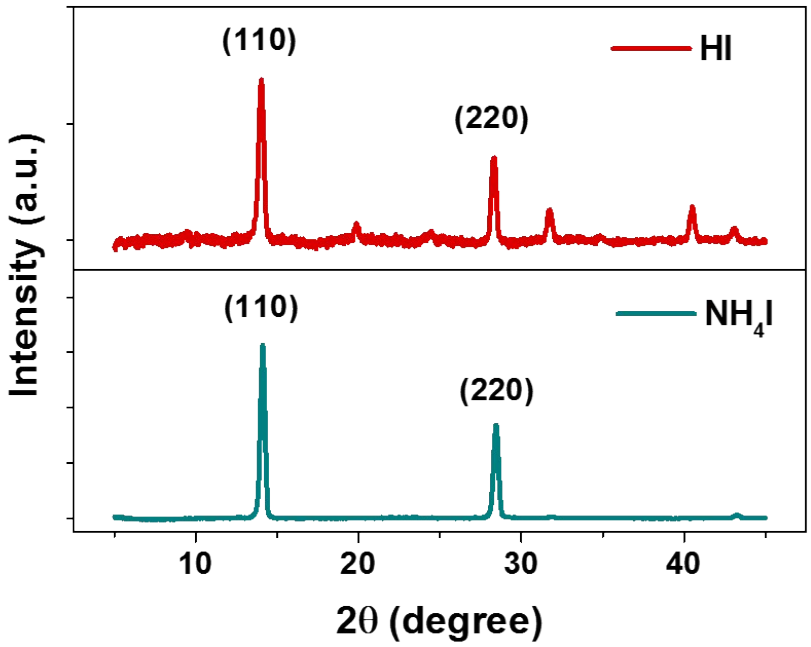

Figure S3. XRD patterns for $MAPbI_3$ thin film processed with a) HI and b) NH_4I

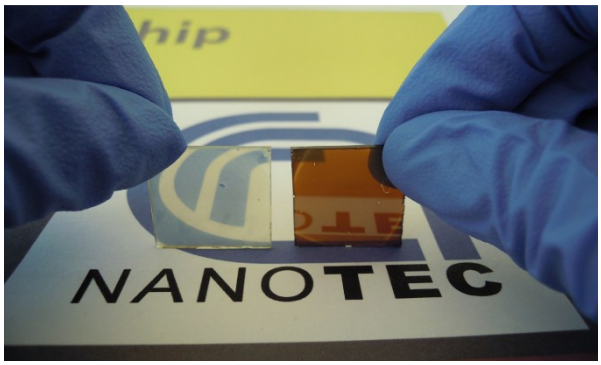

Figure S4. Photograph of $MAPbI_3$ thin film processed with NH_4I additive and exposed to air without performing thermal annealing (left) or after thermal annealing (right).

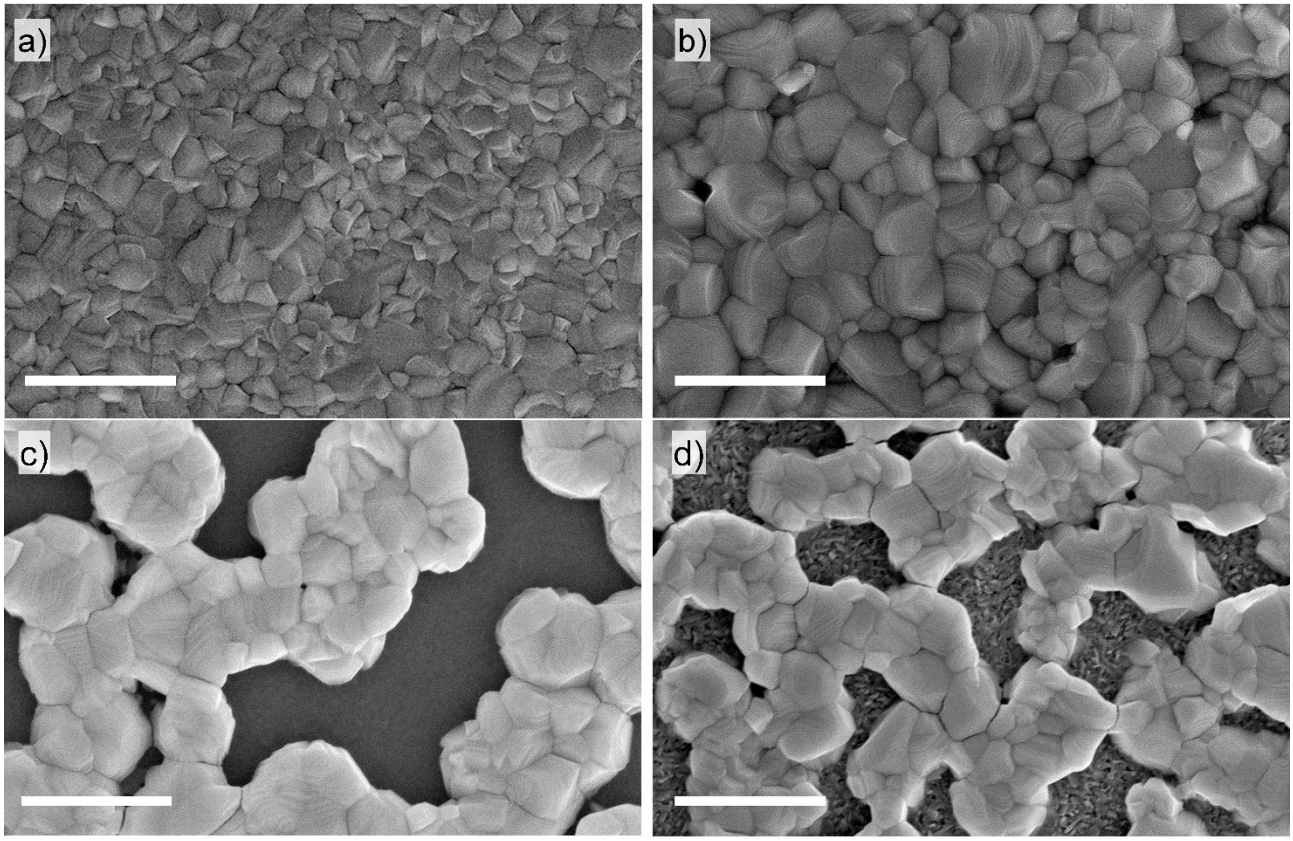

Figure S5. SEM image of $MAPbI_3$ thin film processed with a) HI (HI/PbI_2 molar ratio of 0.3/1) and b) NH_4I (NH_4I/PbI_2 molar ratio of 0.8/1) deposited on TiO_2 substrates. SEM image of $MAPbI_3$ thin film processed with NH_4I (NH_4I/PbI_2) at the same molar ratio used for HI, namely 0.3/1) deposited on c) PEDOT:PSS and d) TiO_2 substrates. Scale bar is 1 µm.

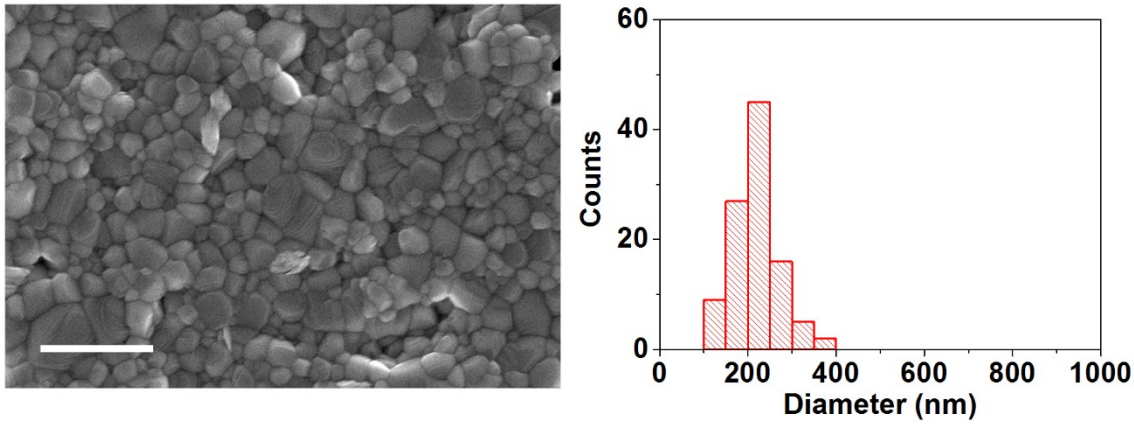

Figure S6. SEM image of $MAPbI_3$ thin film processed with HI by using hot-substrate technique. Scale bar is 1 µm.

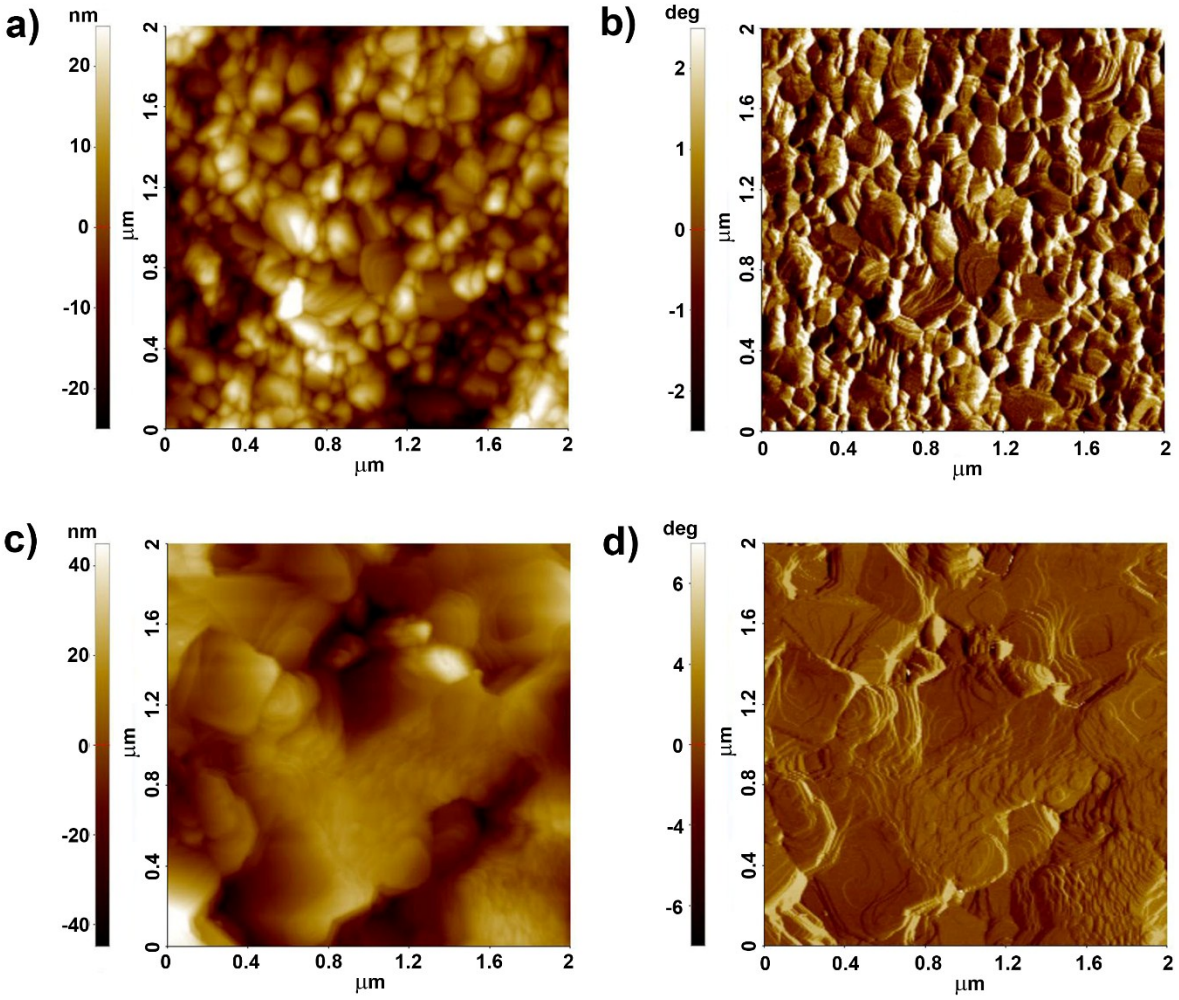

Figure S7. AFM height (left) and phase (right) images of $MAPbI_3$ film on glass/PEDOT:PSS substrates processed with (a-b) HI or (c-d) NH_4I. Rq is 10.1 nm and 13.9 nm for HI and NH_4I, respectively.

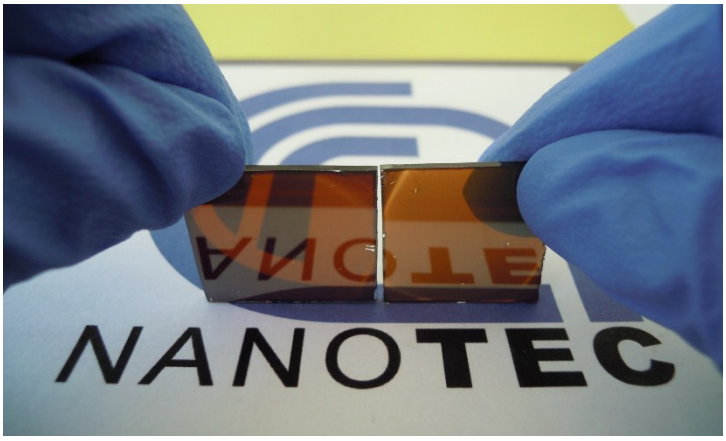

Figure S8. Photograph of $MAPbI_3$ thin film used for device fabrication processed with HI additive (left) or NH_4I (right).

Sample		Jsc (mA/cm^2)	Voc (V)	FF	PCE (%)
HI normal	Forward	16.4	0.92	0.47	7.2
	Reverse	21.3	0.98	0.56	11.8
NH_4I normal	Forward	15.6	0.89	0.45	6.2
	Reverse	17.2	0.96	0.69	11.4
HI inverted	Forward	20.6	0.92	0.72	13.6
	Reverse	21.0	0.93	0.75	14.6
NH_4I inverted	Forward	17.5	0.37	0.46	3.0
	Reverse	17.5	0.40	0.55	3.3

Table S1. Device characteristics of $CH_3NH_3PbI_3$ based solar cells, processed with HI or NH_4I, in forward and reverse scan direction.

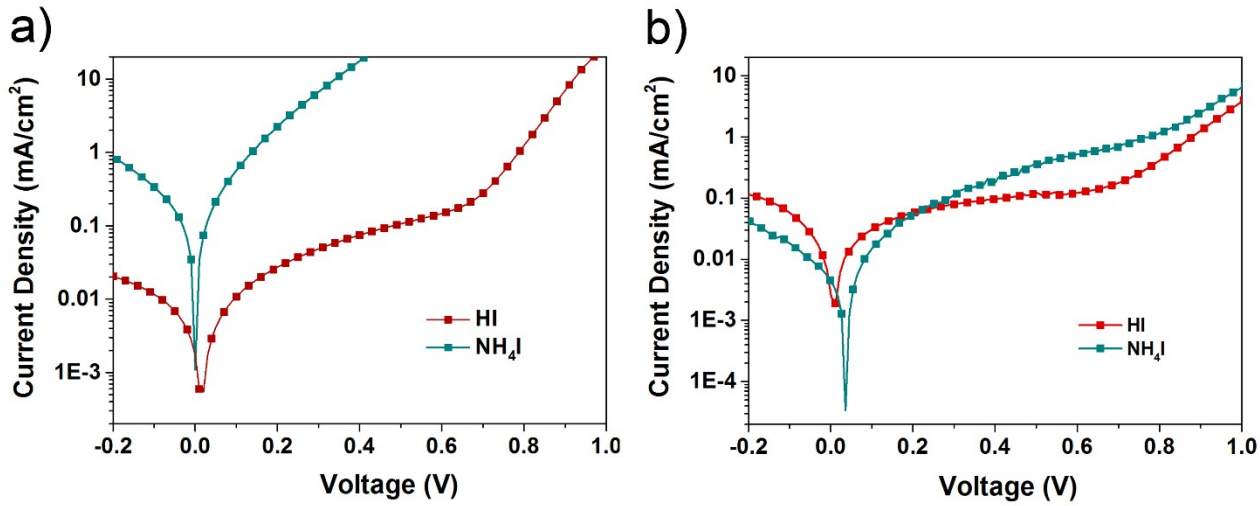

Figure S9 Dark J-V curves of planar heterojunction $CH_3NH_3PbI_3$ solar cells processed with HI or NH_4I additives in a) inverted and b) standard configuration.

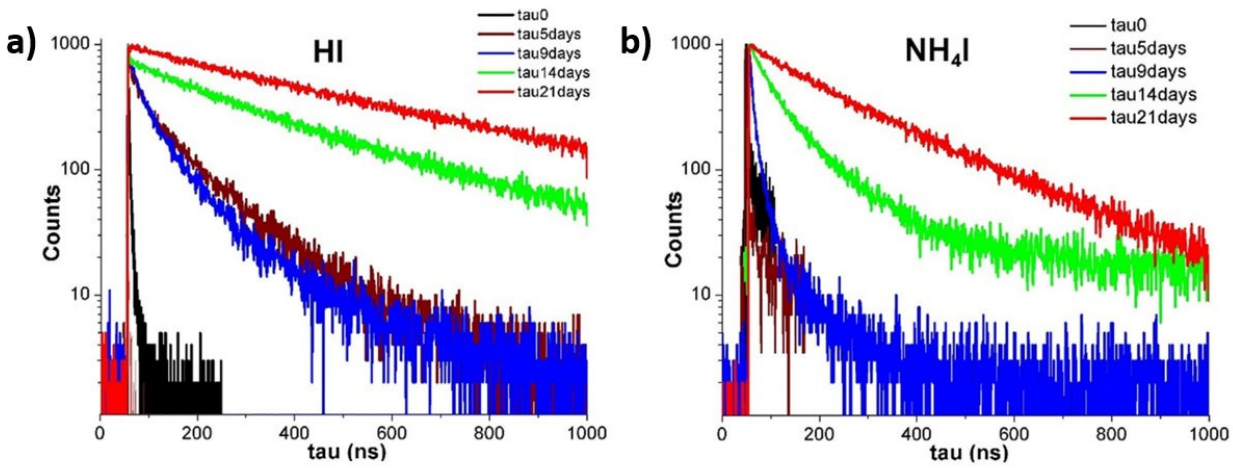

Figure S10. TRPL decays of a) HI-$CH_3NH_3PbI_3$ films recorded at time 0 (**tau0**) and after diverse time intervals (**tau5days**, **tau9days**, **tau14days** and **tau21days**) and of b) NH_4I-$CH_3NH_3PbI_3$ films recorded at time 0 (**tau0**) and after diverse time intervals (**tau5days**, **tau9days**, **tau14days** and **tau21days**) aging was done in air and dark conditions.

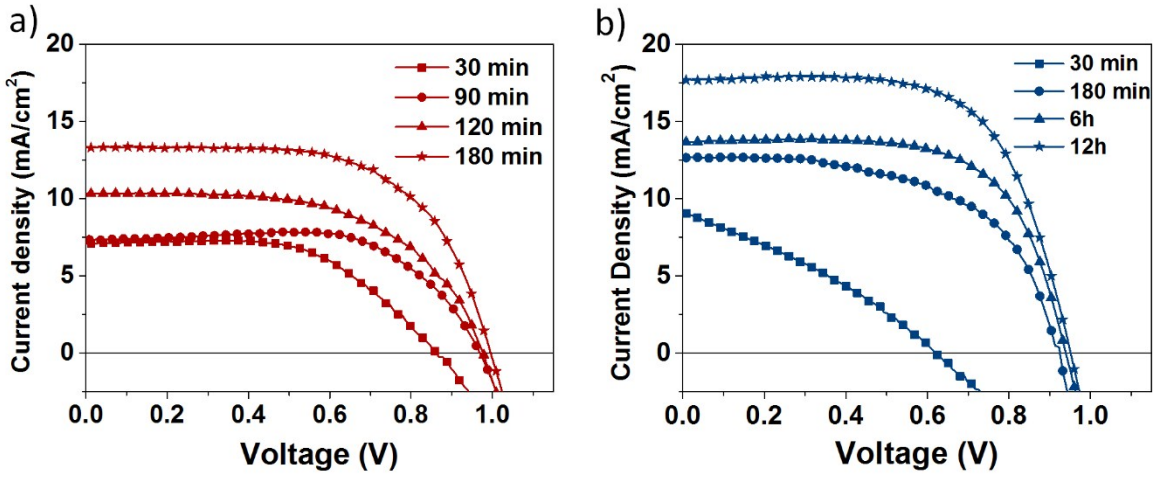

Figure S11. J-V curves of $CH_3NH_3PbI_3$ solar cells in the standard TiO_2 architecture processed with a) HI or b) NH_4I additives exposed for different time to ambient atmosphere.

In order to further investigate and rationalize the effect of ambient atmosphere on HI-$CH_3NH_3PbI_3$ and NH_4I-$CH_3NH_3PbI_3$ films, we prepare $CH_3NH_3PbI_3$ devices in inert atmosphere an then expose them in ambient condition testing the device at different time (corresponding J-V curves are shown in Figure S8 and device parameter listed in Table S2). We can observe that both HI-$CH_3NH_3PbI_3$ and NH_4I-$CH_3NH_3PbI_3$ based devices have a significant increase in FF and Voc increasing the ambient exposure time. The enhancement of performance could be related to a combination of the reduction of trap density in the $CH_3NH_3PbI_3$film, due to air curing, as well as to the Spiro-OMeTAD doping. Still some difference in the behaviour of the two

additive can be observed. HI-$CH_3NH_3PbI_3$ based device reaches the maximum device performance after 3 h of air exposure, which is standard time required for Spiro-OMeTAD doping. This in line with the performance of HI-$CH_3NH_3PbI_3$ in inverted device configuration that do not need any curing to reach high efficiency (Figure S8a). On the other hand, NH_4I-$CH_3NH_3PbI_3$requires 12 h of air exposure to reach the highest performance. Note that, in such test, especially for device with HI, we never reach the maximum performance probably because the repeated measurements on the same device are detrimental for the absolute performances. However, we can clearly observe a trend for which NH_4I- $CH_3NH_3PbI_3$ need longer time of exposure than HI-$CH_3NH_3PbI_3$ to reach the best performance. The longer time evolution of the films for the TRPL (Figure S7) compared to the time required for the curing in the whole device under photovoltaic regime can be ascribed to the different nature of the protective layer, either PMMA or Spiro-OMeTAD respectively having different oxygen/water permeability.

Sample	Air exposure	Jsc (mA/cm^2)	Voc (V)	FF	PCE (%)
HI	30 min	7.1	0.86	0.59	3.6
	90 min	10.3	0.98	0.58	5.9
	120 min	13.1	0.95	0.57	7.0
	180 min	13.3	0.99	0.63	8.4
NH_4I	30 min	9.2	0.62	0.32	1.8
	180 min	12.6	0.96	0.56	6.7
	6h	13.7	0.94	0.66	8.6
	12h	17.7	0.95	0.66	11.1

Table S2. Device characteristics of $CH_3NH_3PbI_3$ based solar cells, processed with HI or NH_4I, exposed for different time to ambient atmosphere.